

Understanding the Physiology and Modelling of the Fontan Pathway

Sachin Talwar*, Tameem Ahmed, Shiv Kumar Choudhary, Sandeep Chauhan
and Balram Airan

Cardiothoracic Centre, All India Institute of Medical Sciences, Ansari Nagar,
New Delhi-110029, India.

*E-mail: sachintalwar@hotmail.com

ABSTRACT

The Fontan operation is considered the final palliation for patients who have a structurally or functionally univentricular heart, that is a condition in which the heart is unable to function in a state where there are two pumps: one for the left side of the heart that pumps the oxygenated blood into the systemic circulation and another for the right side of the heart that pumps blood into the pulmonary circulation (lungs). Although the Fontan operation creates an abnormal physiological environment by dispensing away with the right-sided pump, it has proved to be an important surgical tool to relieve cyanosis and improve the functional capacity of patients who were previously doomed to die. Understandably, it has been studied and evaluated critically and there are constant endeavors to make it better. Engineering and medicine can forge an important partnership in making this operation better. In this review the basic aspects of this operation are discussed along with the role of fluid dynamics to modify this operation as well as help in designing pumps to add energy to this circuit for better long-term outcomes.

INTRODUCTION

The Fontan procedure has been employed as the definitive palliation for a number of congenital heart defects where a serial arrangement of pulmonary and systemic circulations is necessary. [1,2,3]. Since it was first introduced by Fontan and Baudet in 1971, it has undergone many modifications, all of which are aimed at optimizing hemodynamics and preventing the complications of an altered physiology in patients with complex congenital heart disease where a two-pump repair is not feasible and the only viable option is a single ventricle palliation. In essence, these procedures create systemic venous-to-pulmonary arterial “bypass” connections to provide appropriate blood flow to the lungs because the pumping function of the right side of the heart is deficient or not utilized in the circuit. The earliest types of Fontan procedures were accomplished by connecting the right atrium to the pulmonary arteries, the so-called atriopulmonary connections (APC). The pumping action of atrium was considered the prime source for generation of the propelling force for blood in the APC circuit initially [4]. In recent years with insights into the physics and hemodynamics of the Fontan circuit, the efficiency of atrium as a pump in the Fontan circuit came into question [4], and hence there was birth of the different adaptations of Fontan procedure as in the total cavopulmonary connection (TCPC) and its modifications described below, [4, 5, 6]. Currently, many variations to the TCPC Fontan procedure exist. The common theme in all these types of TCPC procedures is the partial or complete exclusion of the atrium from the Fontan circuit. However, the deficiency of a functioning pump on the right side of the heart has the potential to significantly reduce the energy for the forward blood flow towards the pulmonary circulation following a Fontan procedure. Hence, it has always been desirable to introduce modifications of this operation to minimize the energy losses and to improve the forward flow of blood into the pulmonary circulation. It would also seem tempting, yet logical to attempt to modify the conduct of the operation in such a manner that the resulting forward flow is pulsatile. These considerations have necessitated the application of the principles of fluid dynamics and methods to evaluate the Fontan circulation and energy losses. Some of these are briefly reviewed below.

THE FONTAN PRINCIPLE AND ITS MODIFICATIONS

A detailed description of the Fontan operation and its modifications is outside the scope of this review. However, a few basic principles and variations are discussed, as this is crucial to understand the

principles of fluid dynamics as applied to this operation. The principal determinants of the Fontan circulation are unobstructed pathways, with generous connection between systemic veins (superior and inferior vena cava) and the pulmonary arteries, preservation of anatomic and functional integrity of pulmonary vasculature (that includes adequate pulmonary artery size, and normal pulmonary artery pressures and pulmonary vascular resistance) and adequate function of the systemic ventricle (pump) [7]. As schematically shown in Figure 1, broadly, there are three different types of Fontan procedures [8]: (A) Atriopulmonary connection (the original) described by Fontan and Kreutzer, (B) Intra-cardiac total cavopulmonary connection (lateral tunnel) and (C) Extra-cardiac total cavopulmonary connection.

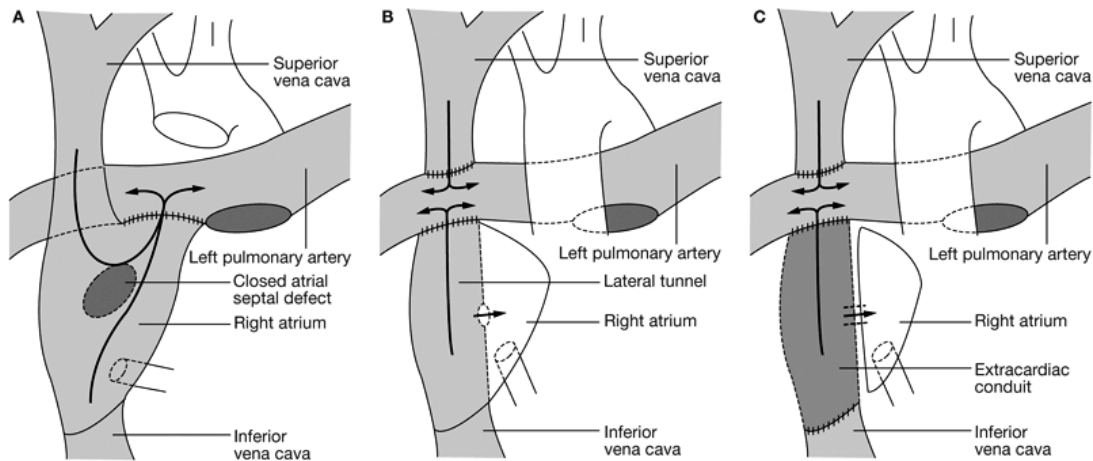


Figure 1. The different types of Fontan circulation (A) Atriopulmonary connection (B) Intra-cardiac total cavopulmonary connection and (C) Extracardiac total Cavopulmonary connection. Reproduced with permission from deLeval MR. The Fontan circulation: a challenge to William Harvey. *Nat Clin Pract Cardiovasc Med*, 2005, 2, 202-208.

In the atriopulmonary connection (A), a direct connection is established between the right atrium and the pulmonary artery. The atrial septal defect is closed and the main pulmonary artery is divided to eliminate the antegrade flow. In the intra-cardiac total cavopulmonary connection (B), an end to side connection is made between the divided superior vena cava and the right pulmonary artery which directs the blood from the head, neck and the upper part of the body into the pulmonary circulation. The inferior vena caval return from the various abdominal organs and the lower extremity is then directed towards the divided cardiac end of the superior vena cava by creating a tunnel within the right atrium using a patch. Following this the cardiac end of the superior vena cava is connected to the undersurface of the right pulmonary artery and this directs all the inferior vena cava return to the pulmonary arteries. The main pulmonary artery is divided to eliminate the antegrade flow. In extra-cardiac total cavopulmonary connection (C), instead of a tunnel inside the heart, a tube graft is interposed between the pulmonary artery and the divided inferior vena cava, the cardiac end of the latter is closed. Therefore the inferior vena caval return follows a course outside the heart via the tube graft to reach the pulmonary arteries and the lungs. The superior vena cava blood comes to the lungs in the usual way as described in (B)

ATRIOPULMONARY CONNECTION

In a normal biventricular (two-pump) circulation the right atrium has four main functions: it acts as a pump, a reservoir, an initiator and propagator of electrical sinus impulse and it has a neurohumoral role of circulatory homeostasis. In an atriopulmonary connection, these functions differ as the right atrium as the right atrium does not empty into a ventricular chamber but directly into the pulmonary arteries. Also, in an atriopulmonary connection, the right atrium acts as a valve less contractile chamber interposed between the systemic venous and pulmonary arterial beds, and thus it operates at significantly higher pressures than normal. It has been demonstrated in vitro that in a simple circuit, depicted in Figure 2, in which underlying flow is maintained by a constant power source, the interposition of a pulsatile valve less chamber does not contribute positively to fluid flow energy. Moreover, pulsations cause an increase

in upstream pressure; the downstream pressure remained unchanged. It has also been shown in vitro, that the interposition of a compliant atrial chamber between the systemic veins and the pulmonary arteries causes loss of energy (Figure 2). Streams of the superior and inferior vena caval blood from opposite directions collide within the atrial chamber, leading to turbulence, and hence energy loss and which is exaggerated by pulsation. Also, due to chronic atrial distension following the traditional atriopulmonary connection, the sinus node and atrioventricular pathway dysfunction occurs which leads to late supraventricular arrhythmias and considerable morbidity.

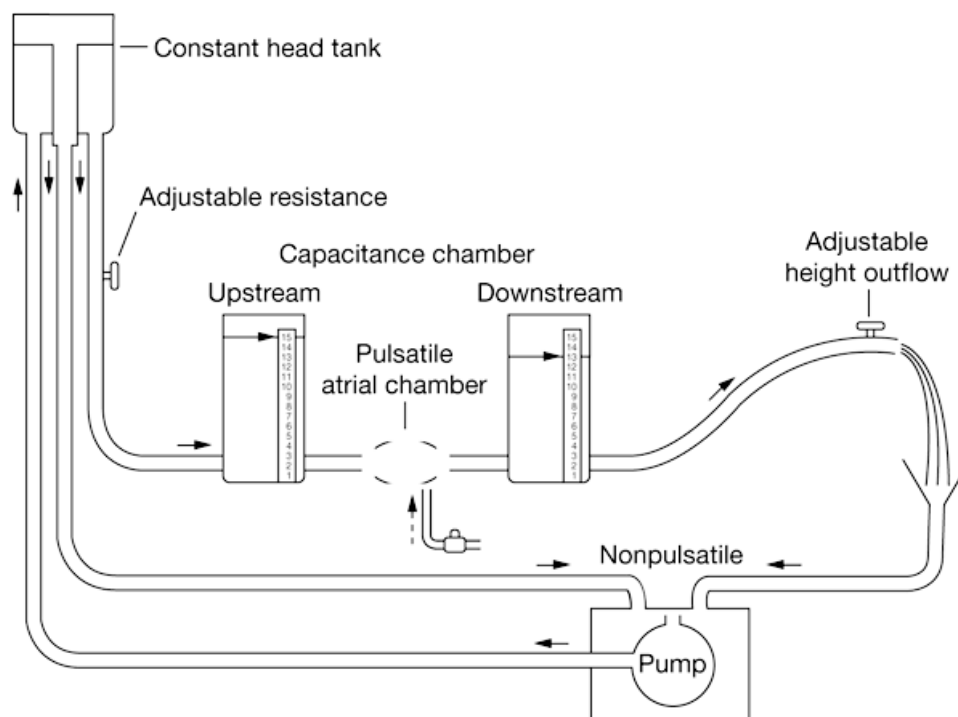


Figure 2. Schematic model of the Fontan circulation. The underlying flow is maintained by a constant power source. The interposition of a valve less chamber, representing the right atrium, does not contribute positively to fluid energy. Moreover, pulsation occurs at the price of an increase in upstream pressure. Reproduced with permission from deLeval MR, The Fontan circulation: a challenge to William Harvey. *Nat Clin Pract Cardiovasc Med*, 2005, 2, 202-208.

It may be pertinent here to discuss the initial experimental models (deLeval et al, 1988) leading to the development of the TCPC. In Vitro studies were designed for this purpose. A suspension of fine aluminum dust in water was used to visualize flow patterns in transparent and in open channels. To study the flow after various surgical procedures, atriopulmonary and cavopulmonary connections were constructed in normal hearts available at autopsy. To measure energy losses, polyester resin casts were made of a series of specifically shaped cavities and corners. These were then connected to 12mm tubing's in a steady flow circuit and pressure losses across the test sections were measured at a range of continuous flow rates. Citrated whole blood instead of water was passed through the test sections. As shown in the figure above, a simple circuit was designed to deliver a steady flow of water through a valveless chamber, representing the Fontan right atrium, which could be made pulsatile or nonpulsatile. The aim of this particular experiment was to observe the effect of introducing pulsation on the pressures upstream and downstream, to record any resistance and or pump like function. Flow was maintained by a constant had tank from a centrifugal pump. The constant head, representing the mean systolic arterial pressure, is kept 100 cm above the level of the atrial chamber throughout the experiment. Using this set-up, a range of mean pressure loss across the chamber was plotted with or without pulsation. A rise in the venous pressure was shown to occur even in the presence of pulsatile energy being put in the system Pressure waves were and altered velocity waves sent both upstream and downstream by the atrial pulsation This simple experiment was the forerunner for a lateral tunnel TCPC.

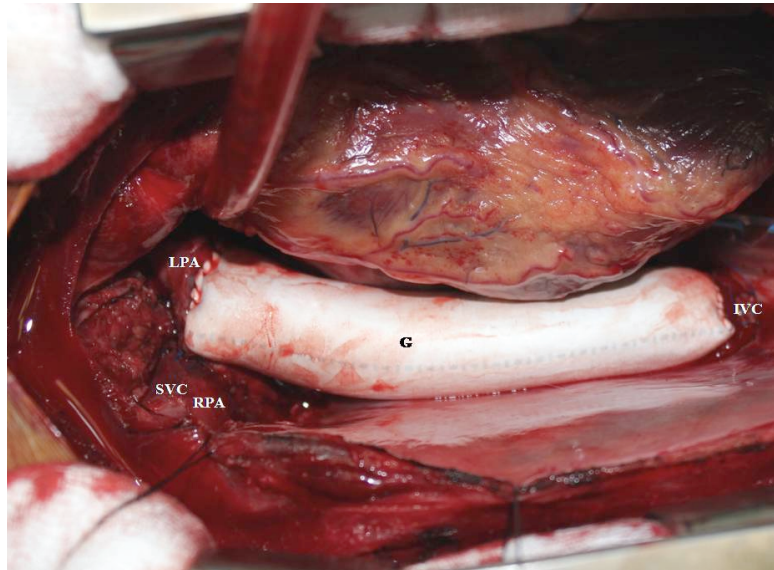


Figure 3. This photograph shows an 18 year old patient with single ventricle physiology undergoing the single-stage Extracardiac Fontan operation using a tube graft (G) connected between the inferior vena cava (IVC) and the right pulmonary artery (RPA). The Superior vena cava (SVC) has also been connected to the RPA. The left pulmonary artery (LPA) is also seen. Please note the relationships of the involved structures: LPA, RPA, SVC and the graft as these have important implications on the flow patterns in the circuit.

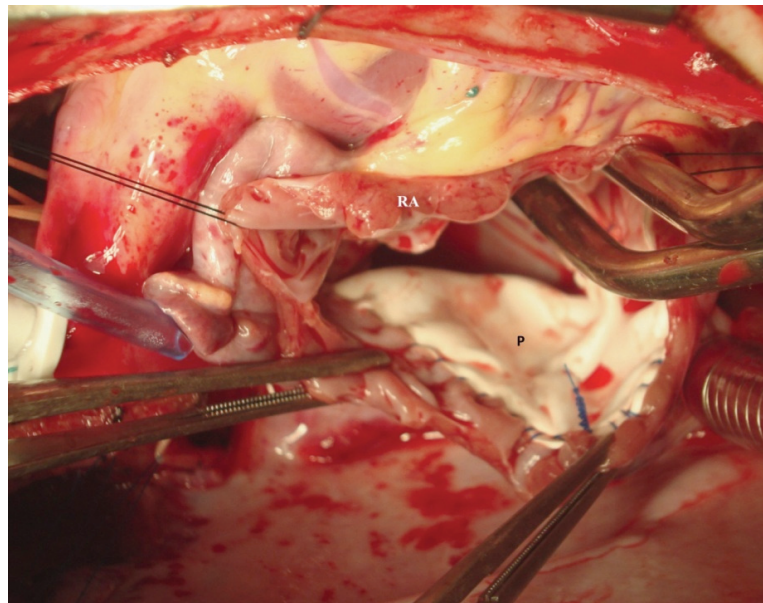


Figure 4. In this operative photograph, 11 years old patient, the lateral tunnel Fontan is being performed. The right atrium (RA) has been opened and a patch of PTFE (P) has been used to direct the inferior vena cava towards the cardiac stump of the superior vena cava.

Total cavopulmonary connection (TCPC)

This procedure diverts the superior vena caval return into the pulmonary arteries and connects the inferior vena cava to the pulmonary arteries. A composite pathway made of the right atrial wall and a prosthetic patch (intra-cardiac total cavopulmonary connection) is created, or an extra-cardiac conduit (extra-cardiac total cavopulmonary connection) is interposed between the inferior vena cava and the right pulmonary artery. The advantages of TCPC are that there is no right atrial distension and therefore a lower incidence of atrial arrhythmias. There is also less turbulence and stasis and less risk of formation of a thrombus in

the right atrium. The TCPC may also be accomplished by placement of an intra-cardiac conduit. However, an intra-cardiac conduit has a higher risk of production of a thrombus leading to systemic embolization as compared to the traditional lateral tunnel Fontan or an extra cardiac conduit. There is an ongoing debate about the superiority of either model above the other, but this is outside the scope of this review.

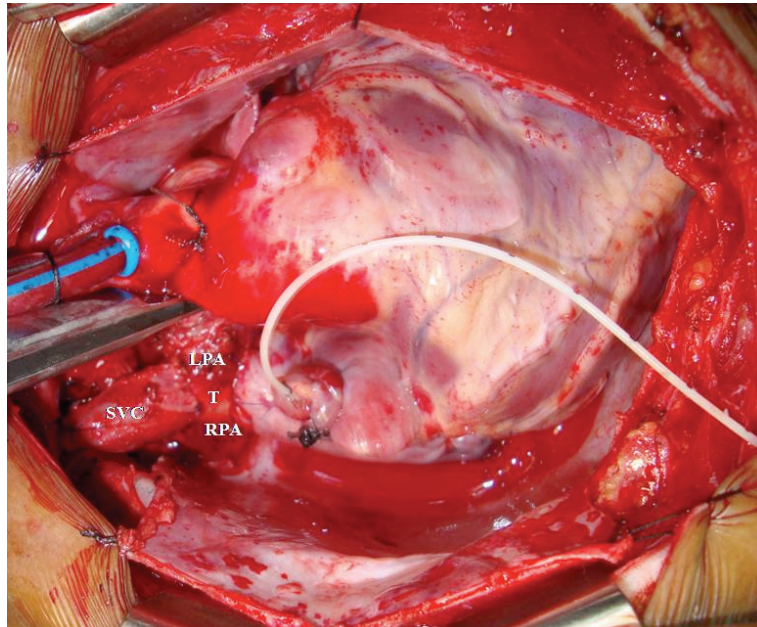


Figure 5. Operative photograph of the completed picture of the lateral tunnel Fontan (shown in Fig. 4) after the right atrium has been closed. The IVC is now draining via the T (which is the cardiac stump of SVC) into the RPA. The SVC is also connected to the RPA. Please note the relationships of the involved structures: LPA, RPA, SVC and the tunnel as these have important implications on the flow patterns in the circuit.

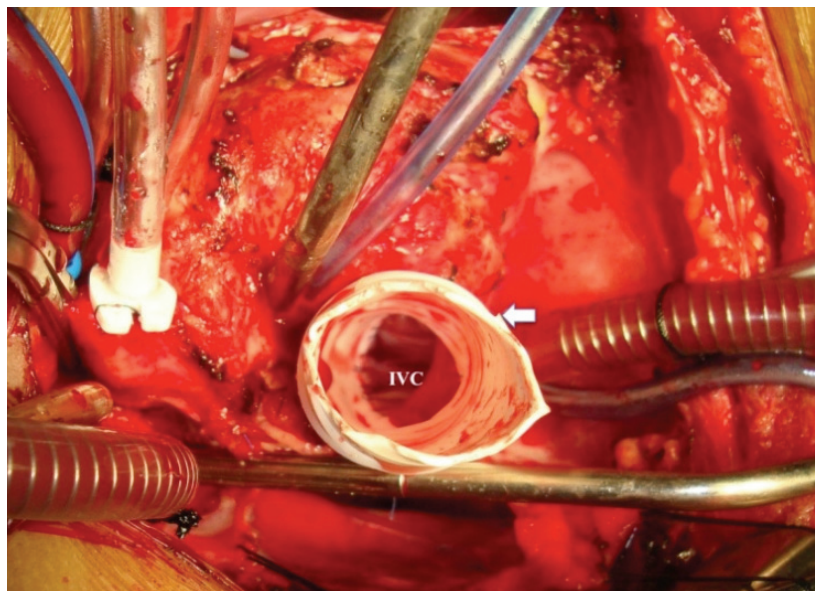


Figure 6. Operative photograph 3 (a): Completion Fontan of the intra-extracardiac type (Lateral tunnel with a tube graft) in a 6-year old patient who has undergone 2 operations earlier: one to reconstruct the left pulmonary artery and another to connect the SVC to the RPA earlier. In this photograph a ringed PTFE tube graft (arrow) has been sutured around the mouth of the IVC.

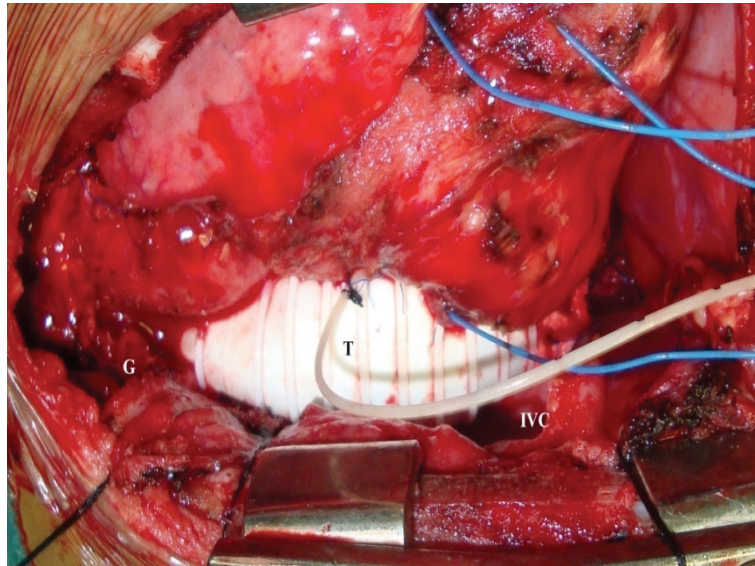


Figure 7. Operative photograph 3 (b): The completed picture of the intra-extracardiac type (Lateral tunnel with a tube graft) of the above patient. The upper end of the graft is sutured to the RPA at the site of the previous Glenn (SVC to RPA anastomosis) labeled as G.

ALTERATIONS IN PHYSIOLOGY FOLLOWING THE FONTAN OPERATION

Knowledge of the alterations in physiology following the Fontan operation gives a better understanding of the goals to be achieved when aiming for or creating an ideal Fontan circulation. These alterations are summarized below under various headings:

The systemic ventricle

The acute preload reduction resulting from the Fontan operation leads to an increase in mass–volume ratio and inappropriate ventricular hypertrophy, and diastolic dysfunction which results in reduced compliance resulting in a rise of the pulmonary venous pressure which is one of the mechanisms leading to a gradual Fontan failure and attrition (8). Experimental and clinical data show that the Fontan circulation is associated with an increase in ventricular afterload and a lack of compensatory increase in contractility. The response of the Fontan circulation to higher ventricular energy requirements is much lower as compared to biventricular circulation. Whereas cardiac output and stroke work are maintained with biventricular circulation by increased ventricular contractility, the same compensatory mechanism does not exist in the Fontan circulation and leads to decreased cardiac output and stroke work.[9-11]

THE PULMONARY CIRCULATION

A higher proportion of total hydraulic power is spent in producing pulsatile flow in the pulmonary circulation than in the systemic circulation [12]. The energy generated by the right ventricle is absorbed by the arterial compliance in systole and restituted in diastole to maintain the patency of the distal vessels [13]. The loss of that energy increases pulmonary vascular impedance and, therefore, afterload. The same lack of energy explains the role of external factors, such as hydrostatic forces and ventilator mechanisms become the key players in the Fontan pulmonary circulation, once the ventriculo-arterial coupling is lost.

THE SYSTEMIC VENOUS RETURN

The serial arrangement of the systemic veins and the pulmonary circulation with its increased pulmonary vascular resistance has a major impact on the systemic venous return. The venous return to the normal heart is classically divided into the superior and inferior vena caval components. The superior vena cava component accounts for 30% of the return and the inferior vena cava for approximately 70%. However, the return is better divided into three subsystems (a) Superior vena cava:

30% (b) systemic inferior vena cava: 45% and (c) Splanchnic system (25%). The latter carries venous blood from the intestine and the spleen, which is collected into the portal vein before it enters the liver and subdivides into a capillary bed (the sinusoids of the liver). The liver sinusoids have the most permeable walls of all the capillary beds in the circulation. This arrangement has important hemodynamic consequences because the liver adds resistance to splanchnic flow. In Fontan patients, gravity has an adverse impact on the return from the inferior vena cava than in a biventricular circulation. Following the Fontan operation, the venous return becomes critically dependent on the forces driven by normal respiration. Therefore any factor that leads to disturbed respiratory mechanics such as a paralyzed diaphragm or obstructive lung disease adversely impacts the Fontan circulation. In an optimally balanced Fontan circuit, there is a definite expiratory augmentation in the flow of blood from the portal venous system towards the pulmonary arteries and this feature starts to disappear once Fontan circulation starts to fail. A combination of stagnation, adverse gravitational factors and capillary leakage ensues that leads to accumulation of fluid in the peritoneal cavity (ascites) and protein losing enteropathy. These changes set up a vicious cycle that is self-propagating and further leads to more stagnation and failure.

THE LYMPHATIC CIRCULATION

As discussed above, the loss of protein via the gastrointestinal tract (Protein-losing enteropathy) results from a reduction in the absorption of lymphatic fluid due to increased venous pressure in the splanchnic territory. The raised pressure in the drainage territory of the superior vena cava is transmitted to the thoracic duct, which increases the lymphatic pressure in the lungs [26, 27] thus producing interstitial pulmonary edema and elevation of pulmonary vascular resistance [14]. This elevation of pulmonary vascular resistance impedes the flow of blood into the pulmonary arteries and is an important factor that aggravates the Fontan failure.

THE COLLATERAL CIRCULATION

Aortopulmonary collaterals in Fontan patients result in significant left-to-right shunt, leading to chronic volume overload of the univentricular heart [15]. Pulmonary arteriovenous fistulae lead to severe systemic arterial desaturation in the Fontan circulation. Both of them are, described mainly in lungs receiving no hepatic blood, hence it has been postulated that the hepatic factor, potentially prevents the development of these fistulae (16). The pressure difference between the systemic and the pulmonary veins in the Fontan circulation can open up small collateral vessels (17) that connect naturally the systemic mediastinal veins and the pulmonary veins. This is another potential mechanism for progressive and increasing cyanosis in the late Fontan patient. Progressive late systemic arterial desaturation is sometimes noted in patients in whom the systemic venous pathway is fenestrated. Progressive increase in pulmonary vascular resistance could account for the progressive nature of this cyanosis.

WHAT IS AN IDEAL FONTAN?

In a normal biventricular circulation the mean caval pressures are less than 10 mmHg and the mean pulmonary arterial pressure is at least 15 mmHg to keep the pulmonary vasculature patent. In the Fontan circulation there is caval hypertension—particularly in the splanchnic area and relative pulmonary arterial hypotension. This is “Fontan Paradox”. In pure hemodynamic terms, a mechanical device capable of producing a step down in pressure energy of 5 mmHg in the inferior vena cava and producing a step up of 5 mmHg in the pulmonary arteries could potentially reverse the Fontan paradox and any system or power generator which can reverse this paradox can serve to prevent Fontan failure.

The clinical problem presented to the cardiac surgeon is to design a cavopulmonary connection with (1) minimal energy losses avoiding even minimal gradients, areas of stagnation, and “right angles”; (2) potential for growth, and (3) equal vena cava and hepatic vein distribution to both lungs [18]. Despite attempts to optimize the Fontan circulation, the basic physiology remains: pulmonary and systemic vascular resistances are in series and venous return is devoid of a high-energy hydraulic power source. In such a circulatory arrangement, where venous return and pulmonary perfusion occur in a low energy state, maximizing energy conservation assumes significance [19]. A hemodynamically inefficient Fontan circulation would thus result in increased energy loss with venous hypertension and congestion as discussed above [20-21]. Resistance to blood flow in a low energy system is critically dependent on the geometry of the circuit, where friction and power losses occur due to connections with abrupt

bends, junctions, and expansions. Therefore, much work has been focused on achieving the energetically optimal Fontan geometry that minimizes venous hypertension, yet still provides satisfactory pulmonary perfusion [22-42].

ATTAINING AN IDEAL FONTAN

Since the early days of the Fontan procedure, there has been a quest to attain an ideal and balanced Fontan circulation. In Vivo, in vitro and computational techniques have been used to elucidate the unique and intriguing hemodynamics of the Fontan pathway. It is hoped that the application of these technological advances will serve to improve the efficiency of the Fontan circuit and extend the quality and quantity of life of patients subjected to this procedure because of a lack of a normal biventricular configuration. [43,44]. Attaining an “ideal” Fontan procedure requires the following (a) minimize abnormal blood flow types including turbulence, vortices, high shear stresses, separation of flows, recirculation, and areas of stagnation. These factors dissipate energy and may induce thrombosis. (b) Ideal Fontan should supply the lungs with appropriate blood flow sufficient to guarantee adequate oxygenation and also provide equal distribution of blood flow from IVC to both lungs (c). Furthermore, anatomic considerations that can indirectly affect the Fontan patient’s hemodynamic status need to be considered, including differences in the incidence of atrial arrhythmias among patients with a TCPC lateral tunnel versus an extracardiac conduit [45]. Achievement of these goals requires a delicate balancing act because an optimal change in one of the components of the circuit may adversely impact the other component. [46].

APPLYING COMPUTATIONAL FLUID DYNAMICS IN FONTAN CIRCULATION

Computational fluid dynamics (CFD) techniques are among the most powerful tools available to the engineering branches dealing with the motion of fluids and exchange of mass, momentum and energy. The utilization of computational fluid dynamics (CFD) as a scientific tool was limited in the past because the governing equations (Navier–Stokes) were too complicated to solve for practical hemodynamic models. As faster and more powerful computers have become available, it has become practical to replace the complex formulas and use CFD in the study of the Fontan circulation. Advantages of CFD over in vitro models are the easy quantification of hemodynamic variables (such as flow rate, pressure, shear stress distribution) and changes in geometric and fluid dynamics parameters. CFD methods allow the development of 3-D models that can reproduce both the complex anatomy of the investigated region and the details of the surgical reconstruction, especially with the developments in magnetic resonance imaging. In addition, CFD models enable one to obtain the solution of the non-linear equations governing the motion of blood in vessels with proper boundary and initial conditions. Thus CFD provides solutions of the Navier Stokes equations.

Navier-Stokes equations

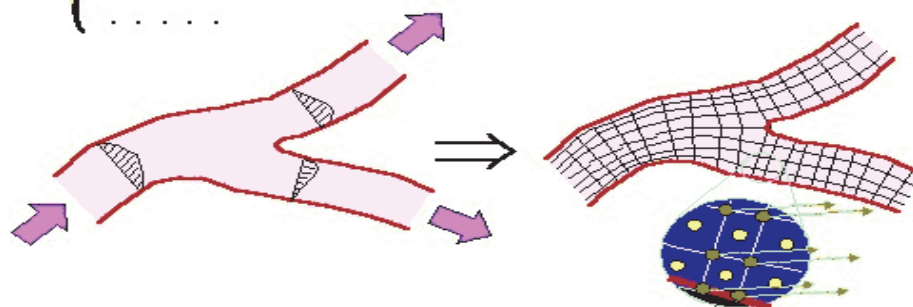
$$\left\{ \begin{array}{l} \rho \left\{ \left(\frac{\partial \mathbf{v}_x}{\partial t} \right) + v_x \frac{\partial \mathbf{v}_x}{\partial x} + v_y \frac{\partial \mathbf{v}_x}{\partial y} + v_z \frac{\partial \mathbf{v}_x}{\partial z} \right\} = F_x - \frac{\partial p}{\partial x} + \mu \nabla^2 \mathbf{v}_x \\ \dots \dots \dots \\ \dots \dots \dots \end{array} \right.$$


Figure 8. Computational techniques provide a solution of the Navier-Stokes equations. Reproduced from Migliavacca F, Dubini G, deLeval MR. Computational fluid dynamics in paediatric cardiac surgery. *Images Paediatr Cardiol*, 2000, 2, 11-25.

MATHEMATICAL MODELS

Fluid dynamics in great arteries can be described by equations of mass and momentum conservation (Navier-Stokes equations) when the non Newtonian features of blood can be ignored [19]. Basically, these are partial derivative equations, which can be analytically solved only for simple cases when the boundary conditions are properly set. CFD techniques, among which the finite element method, allow one to solve the fluid dynamic field in most of the cases where the analytical solution cannot be achieved. The first step in creating a three-dimensional CFD model is to reproduce the geometry of the investigated region and to divide a continuum in a number of simple element ('bricks') where the unknowns of the problem (pressure and velocity) will be evaluated. Geometric data are obtained from angiograms, MR images, Doppler measurements, etc. Imposition of the boundary conditions (i.e. velocity and pressures at the inlets and outlets of the model) is the second step. The mathematical code adopted then will calculate the fluid dynamic field. The last step is the analysis of the results. These methodological steps for the construction and analysis of fluid dynamics in 3-D models are given in Table 1 and Figure 9.

Table 1. Methodological steps for the construction and analysis of fluid dynamics in 3-D models

- Reproduction of the geometry of the investigated region
- Division of the fluid domain continuum in a number of simple elements ('bricks')
- Imposition of the boundary conditions at the inlets and outlets
- Calculation of the fluid dynamic field
- Analysis of the results

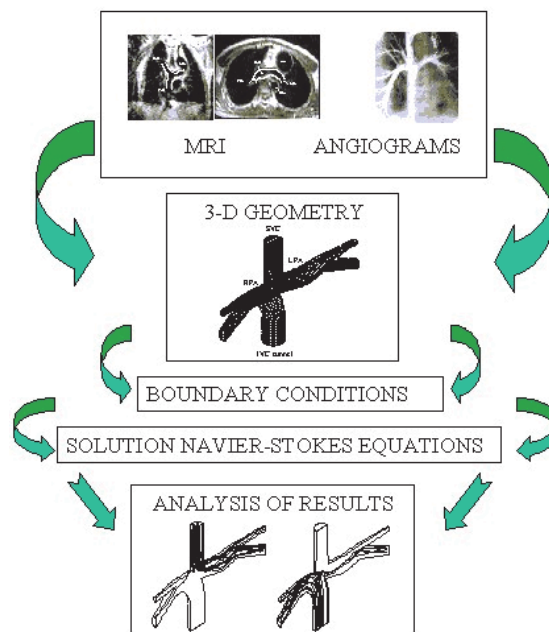


Figure 9. Methodological steps for the construction and analysis of fluid dynamics (see Table 1) in 3-D models. Reproduced from Migliavacca F, Dubini G, deLeval MR. Computational fluid dynamics in paediatric cardiac surgery. *Images Paediatr Cardiol*, 2000, 2, 11-25.

The advantages of 3-D models for studying the various circuits is that it allows one to describe in great detail fluid dynamics in specific portions of the circuit and the cardiac territory. However, the physiological effects of these features on global hemodynamics such as cardiac output and pulmonary-to-systemic flow ratio cannot be studied using 3-D models. To gain this information, lumped parameter models or electrical analogue are required. Different types of these models are listed in Table 2.

Table 2 Summary of various models in the literature for studying the Fontan Circulation

Author and year	Model types	Vessel shape	Inlet BCs	Outflow BCs	Model flow rates (L/min)	Flow Ratios Different and/or in:	SVC —IVC (OS, AN, PL, FL)
Amodeo et al. 2004	TCPC-EC	TB	ST	NS	1,2,3,4	SVC/IVC/RPA/LPA	OS,AN
Bove et al. 2003	TCPC-EC,TCPC-IC, .BDG, HF	AN	PU	SG	2.23	SVC /IVC	OS,AN,PL
De Zelicourt et al. 2005	TCPC-IC	TB,AN	ST	LP	1,2,3,4	SVC/IVC/LPA/RPA	N/A
DeGroff et al. 2005	TCPC-IC	TB	ST	SG	2	SVC/ICV	OS
DeGroff & Shandas 2002	TCPC-IC	TB	ST	SP,PU	2	N/A	OS
Grigioni et al. 2005	TCPC-EC	TB	ST	SP	3	SVC/ICV	OS,AN
Guadagni et al. 2001	HF	AN	ST	LP	0.5,1,2	LPA/RPA	N/A
Healy et al. 2001	BDG, TCPC-EC	TB	ST	SP	2	SVC/IVC/LPA/RPA	FL
Hsia et al. 2004	TCPC-IC, EC	AN	ST	SP	1.65	SVC/IVC	FLTCPC
Khunatorn et al. 2002	TCPC	TB	ST	SP	2	SVC/IVC	OS
Liu et al. 2004	TCPC-EC	TB	ST	SP	4	SVC/IVC/LPA/RPA	PL
Masters et al. 2004	TCPC	TB	ST	LP	1.3	N/A	OS
Migliavacca et al. 2003	TCPC-IC,TCPC-EC	AN	PU	SG	2.3	N/A	FL
Moyle et al. 2006	APC,TCPC	AN	ST,PU	SP	NS	NS	N/A
Orlando et al. [2005	TUBE	TB	PU	SP	N/A	N/A	N/A
Orlando et al. 2006	TCPC	TB	PU	SP	2.5	SVC/IVC	N/A
Pekkan et al. 2005	TCPC-IC	AN	ST	SP	1-3	SVC/IVC/LPA/RPA	PL
Pekkan et al. 2007	TCPC	BOTH	PU	LP	NS	N/A	N/A
Ryu et al. 2001	TCPC	TB	ST	SP	4	SVC/IVC/LPA/RPA	OS,PL
Socci et al. 2005	TCPC-IC	AN	ST	SP	3.6	SVC/IVC/LPA/RPA	N/A

This table has been adapted from: DeGroff CG. Modeling the Fontan Circulation: where we are and where we need to go. *Pediatr Cardiol*, 2008, 29, 3-12.

Amodeo et al., De Zelicourt et al. and Ryu et al. have described IVT models; rests are CFD models. All models except Amodeo et al., Healy et al., Masters et al. and Ryu et al. are true 3D CFD models. The model of Maters et al. and Orlando et al. are with compliance, rests are not.

ABBREVIATIONS	DEFINITION
AN	Angle
APC	Atriopulmonary connections
BDG	bidirectional Glenn
CFD	computational fluid dynamics
FL	flaring of IVC ,/SVC junction
HF/HFP	hemifontan
IVT	IN VITRO
LP	lumped parameter
OS	Offset
PL	planarity
PU	pulsatile flow
SG	sponge
SP	simple pressure
ST	steady flow
TB	Tube shapes
TCPC - EC	TCPC extra cardiac
TCPC - IC	TCPC intra cardiac

LUMPED PARAMETER MODELS

These models are based on the principle of analogy between hemodynamics and electricity. As a result, the circulatory system is modeled as a hydraulic network composed of resistance, inertance and compliance elements as well as non-linear resistance components that incorporate energy losses at the connections. If pressure gradient is analogous to voltage, flow to current, compliance to capacitance, inertance to inductance and hydraulic resistance to electrical resistance, equations of electrical network can be applied and the effects of any changes in the system parameters calculated [30]. The figure below provides an example of the bidirectional cavopulmonary anastomosis (BCPA) which is the anastomosis of the superior vena cava to the right pulmonary artery.

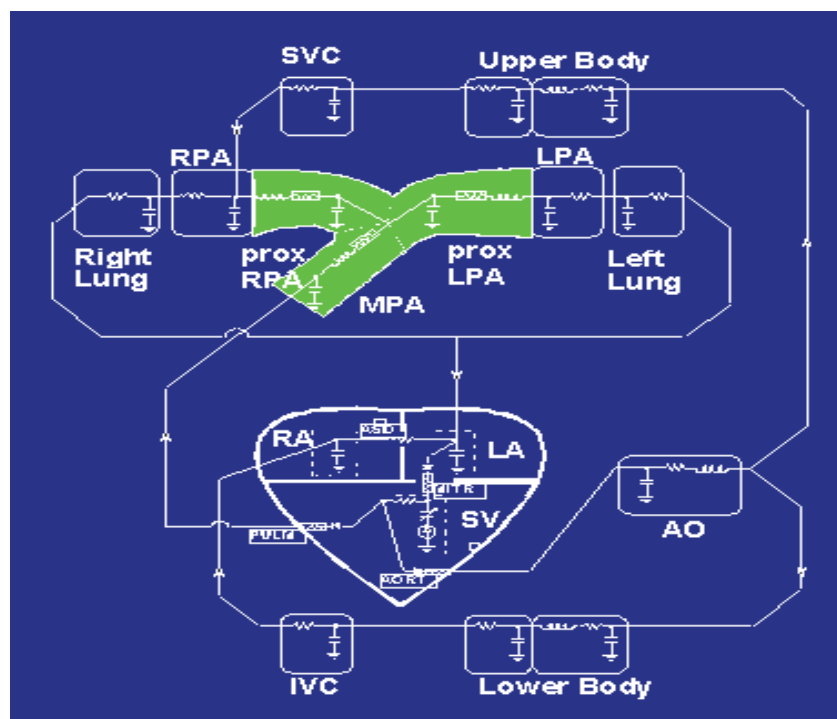


Figure 10. Lumped parameter model of BCPA circulations. Green area includes results of 3-D models. Reproduced from Migliavacca F, Dubini G, de Leval MR. Computational fluid dynamics in paediatric cardiac surgery. *Images Paediatr Cardiol*, 2000, 2, 11-25.

The systemic circulation consists of an RCL block representing the ascending aorta and the two parallel upper and lower body branches. Each parallel branch is assumed to be divided into three stages, which represent the arterial compartments, the venous compartments of the upper and the lower body and the venae cavae, respectively. The upper body branch is connected with the pulmonary circulation by means of an end-to-side anastomosis between the superior vena cava and the right pulmonary artery, while the lower body branch is connected to the heart with a compliance element representing the right atrium. The modeled pulmonary circulation looks rather similar to the systemic one, but it is conceptually different. More precise detail is required at the level of pulmonary arteries in order to incorporate properly the effects due to the surgical repair. A RC block (right and left lung) representing the right and left lungs with their veins completes each pulmonary branch, which eventually delivers blood into the left atrium. 3-D models of BCPA emphasize the impact of local geometry on fluid dynamics [11]. Results of lumped parameter model are fairly consistent and are in agreement with clinical data.

CREATION OF FINITE ELEMENT METHOD MODEL

One of the most commonly used methods in computational fluid dynamics (CFD) to create the model of the Fontan circulation is the finite-element method (FEM). Here, the mathematic equations (Navier-Stokes equations) are replaced by algebraic equations so that a computer is used to obtain the solution. This process of converting the continuous model into a discrete model of algebraic equations is called discretization. All methods of discretization involve making an estimate that approaches the true continuum solution. This is liable to happen as the number of discrete variables increases. The FEM is therefore a method of discretization where the flow domain is divided into a number of simply shaped regions called finite elements. Within each element, a certain number of points or nodes are defined where the numeric value of the unknown functions, and eventually their derivatives, will have to be determined. This concept of FEM is schematically illustrated in Figure 6. The space discretization consists in setting up a mesh or a grid in which the continuum of space is replaced by a finite number of elements.

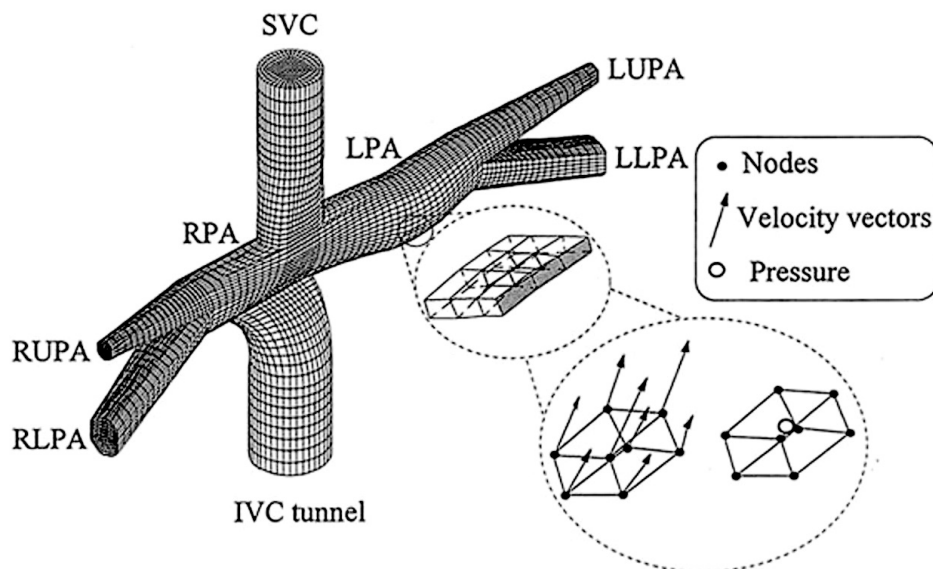


Figure 11. Diagram of an FEM mesh of the TCPC model. The insets show the finite elements with low presentation of an eight-node (three-dimensional) isoparametric brick element with locations for velocity vectors and for pressure calculation in another element. LUPA, Left upper pulmonary artery; LLPA, left lower pulmonary artery; RUPA, right upper pulmonary artery; RLPA, right lower pulmonary artery. Reproduced with permission from de Leval MR, Dubini G, Migliavacca F, et al. Use of computational fluid dynamics in the design of surgical procedures: application to the study of competitive flows in cavo-pulmonary connections. *J Thorac Cardiovasc Surg*, 1996, 111, 502–513.

The figure below demonstrates the flow and velocity patterns by the particle plot paths in flow motion in various types of Fontan as modeled by CFD. The information provided by such models helps the surgeons to evaluate the effects of offsetting and flaring cavopulmonary connections at varying pulmonary flow ratios to determine the optimal geometry of the connection. For the surgeon, conducting the operation to achieve either of these variants is not difficult, but CFD modeling tells us that the construction of each type of connection has different end result and alters the physiology advantageously in certain types. In this very study as depicted in the figure below, the Lateral Tunnel Fontan performed after a previous Hemi Fontan operation (HFP) was found to confer a significant hemodynamic advantage. Both types of completion Fontan techniques after the BDG, the TCPC and the ECC, are associated with higher energy losses, greater vena caval pressures, and less balanced IVC FD between the two lungs. The IVC flow into the pulmonary arteries is evenly distributed in the LT Fontan model, whereas the TCPC and ECC models exhibit preferential perfusion to the left lung, an effect most notable with the ECC model. Modeling the TCPC and the ECC with patches or beveling to either side reduced but did not eliminate these differences and could not guarantee a balanced IVC FD. Although the explanation for these findings is not immediately apparent from this study, the hemodynamic advantage obtained by the caval offset is probably involved. When either the TCPC or the ECC is performed after a BDG anastomosis, caval offset is achieved by beveling the IVC portion of the connection to either the right or left lung. As demonstrated in this study, beveling the TCPC to the right conferred a significant advantage to the TCPC. Similarly, when the ECC was beveled toward the left lung; important differences were found in FD but not power losses. In contrast, the HFP provided a consistent caval offset in an antero-posterior direction because the IVC flow is directed anterior to that of the SVC. The LT connection is independent of that relationship. Although the exact performance characteristics of the TCPC and ECC procedures have important implications for efficiency of design, space constraints limit the surgeon's ability to offset the two caval return pathways to the maximum advantage.

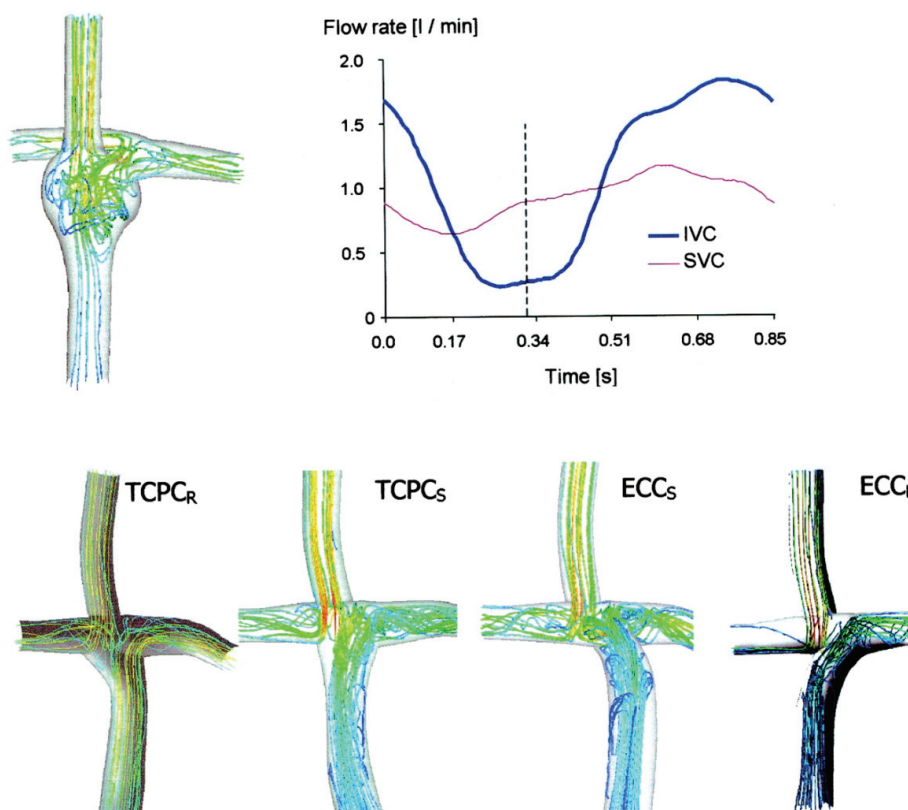


Figure 12. Path lines at 0.3 seconds (see time function plot, upper right panel) corresponding to simultaneous SVC and IVC injections for completion Lateral Tunnel Fontan (upper left panel) and TCPC with patch to right (TCPC_R), straight TCPC without patch (TCPC_S), straight ECC without bevel (ECC_S), and ECC with bevel to left (ECC_L). Reproduced with permission from Bove E. L. et al.; J Thorac Cardiovasc Surg, 2003, 126, 1040-1047.

THE AREAS OF COMPARISON AND STUDIES IN CFD

The advantages of the CFD modeling for studying univentricular physiology are (a) Comparison between different types of TCPC procedures [34, 35, 36, 37] (b) Assessment of the size and shape of the TCPC vessels and the size and shape of their anastomosis [38, 39, 40, 41, 42, 43, 44, 45], (c) The caval anastomosis offset [46, 47], (d) the angle of the anastomosis, and (e) The planarity of the TCPC vessels [48, 49, 50]. Not only this, various flow states and haemodynamic conditions can be studied in various models and include (a) flow distribution between left pulmonary artery (LPA) and right pulmonary artery (RPA), (b) SVC–IVC flow rate ratio, (c) steady versus pulsatile blood flow, (d) SVC/IVC/LPA/RPA velocity profiles, (e) reverse blood flow, (d) additional sources of blood flow and (f) pulmonary artery pressure changes.

LIMITATIONS OF CFD

In spite of their advantages and contributions to the understanding of the univentricular physiology, the CFD models have their inherent limitations. Comprehensive validation in terms of clinical data from modeling is not provided in majority of the studies. A major limitation is a wide range of anatomical variations that are encountered in patients with single ventricle physiology such as anomalies of cardiac position, systemic and pulmonary venous drainage and associated lesions which are nearly impossible to mimic. In addition, significant assumptions have to be made to simplify the analysis and therefore, this covers only a small sample of the anatomic and physiologic conditions. Moreover, the model vessel wall is often assumed to be a non-compliant tube which is far from true for the human circulation.

The other important physiological factor that seriously impacts the Fontan circulation is the effect of respiration on the flow fields and this is ignored during CFD and the flow is typically assumed to be steady and nonpulsatile [29]. Lastly, studies that encompass different age groups and different hemodynamics are not available and extremely few studies show the patterns of flow in resting and exercise states in these patients.

THE FUTURE OF THE COMPUTATIONAL MODELS

Having initiated a discussion on the need, mechanisms, applications and limitations of the various CFD models, it is logical to now plan for the future to derive maximum benefits from the progress that has been made so far and to progress this science further. Some of the innovations are required to (a) create models with vessel diameters and flow rates representative of the range seen in the patient group under study including resting and exercise states, (b) ensure appropriate matching of the vessels shape, sizes and flow rates, (c) model the vessels as compliant structures and not as rigid tubes, (d) accurately model the surgical anastomotic sites and the surgical material used, (e) model different flow patterns which may not be steady all the time (f) account for the effects of respiration and finally create models of all the possible modifications and help to shape the anastomosis further.

APPLICATIONS OF CFD IN TREATMENT OF THE FAILING FONTAN

As discussed above, the Fontan circulation is an unphysiological state, which is doomed to fail with the passage of time. Because of the interdependence and delicate interplay of multiple factors, this state is not self-limiting and responds poorly to medical manipulation by drugs. Rather the failure is self-propagating and the only hope for survival in these patients is then a dramatic alteration in the physiology. The traditional treatment options for this group are limited and have limited benefits to offer. For example, diuretic therapy may alleviate symptoms of increased tissue water, but at the expense of circulating blood volume. An ideal therapy for such patients would be to simply reduce systemic venous pressure alone. Similarly, inotropic drugs improve the cardiac output inefficiently in an under filled ventricle, so ideal therapy would be to simply increase ventricular filling. This has led to the principle of Cavopulmonary assist, which can ideally and concurrently address both of these issues. CFD studies are needed to design and to see the applicability of such assist devices in the Fontan circuit. CFD studies are also needed to validate the role of existing ventricular assist devices in a univentricular hearts as opposed to biventricular circulation and help to design miniature assist devices, which can easily be implanted within the venous pathway and help to propel blood towards the pulmonary arteries.

This model shown below shows the application of Computational fluid dynamics in simulating flow in Fontan circuit with microaxial pumps and viscous impeller pumps for a failing Fontan circulation. The authors of this report hypothesized that a viscous impeller pump, based on the von Karman viscous

pump principle [51] may possess qualities that are ideal to serve in this capacity. The impeller is capable of inducing a pressure increase of 0 to 20 mm Hg and flow rates of 0 to 5 L/min at rotational speeds of 0 to 7K rpm. No reduction in flow rate was observed at 0 rpm, and no gross cavitation was observed at 7K rpm. Performance curves of this device are characteristically flat, signifying consistent low-pressure performance over a wide range of flow conditions. At high pump speeds, the device can generate pressure increase that is greater than the 2 to 5 mm Hg optimum range because of the presence of surface vanes. Lower pressure increase values can be obtained at lower pump speeds or by using a more smoothly surfaced impeller (lower profile surface vanes). The operational speed of the pump and extent of surface vane expression may vary depending on the clinical conditions in which the pump is applied. The use of surface vanes to modify impeller performance must be balanced with acceptable shear rates at defined operational specifications. It is anticipated that many more such unique models will be created and help in our understanding of how to achieve the best long term outcomes for these patients while simulating the natural mechanisms as closely as possible.

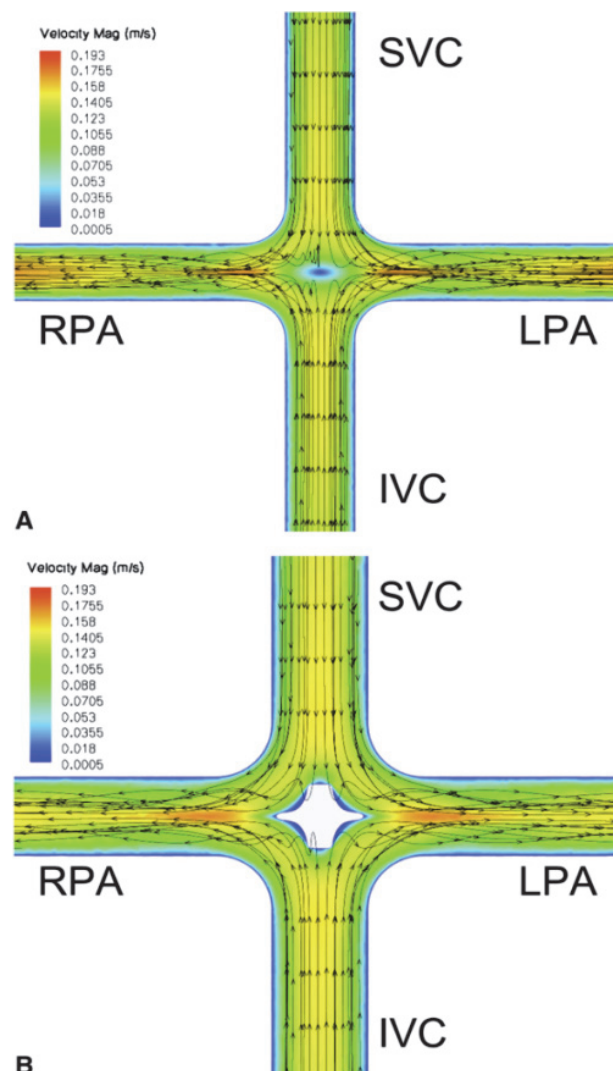


Figure 13. Velocity magnitude (m/s) contour plot within the TCPC at flow of 4.4 L/min. A, No impeller. Incoming flow is irregular at the intersection. B, Stationary impeller. Flow pattern is stabilized, reducing power loss by 88%. SVC, Superior vena cava; IVC, inferior vena cava, LPA, left pulmonary artery; RPA, right pulmonary artery. Reproduced with permission from Rodefeld et al. *J Thorac Cardiovasc Surg*, 2010, 140, 529-36.

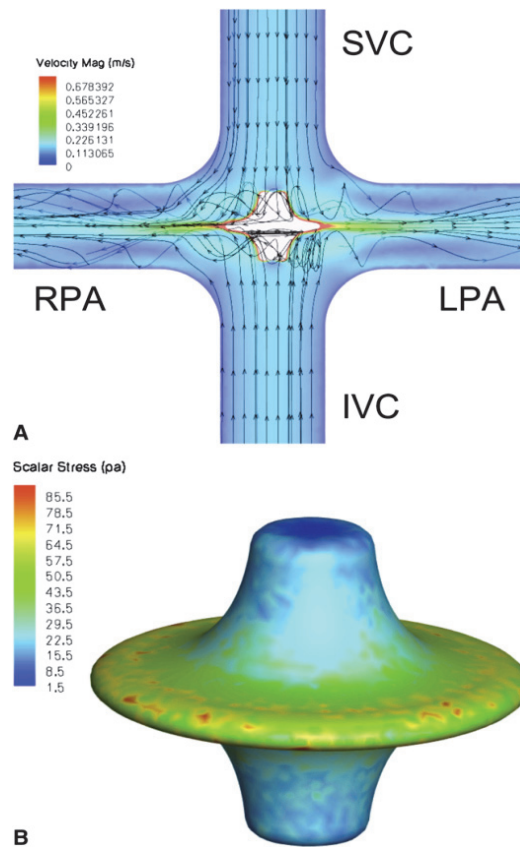


Figure 14. Predicted scalar stress (Pa) (A) and fluid streamlines as colored by total pressure (Pa) (B) for a smooth surface viscous impeller pump rotating at 5000 rpm. SVC, Superior vena cava; IVC, inferior vena cava, LPA, left pulmonary artery; RPA, right pulmonary artery. Predicted scalar stress (Pa) (A) and fluid streamlines as colored by total pressure (Pa) (B) for a smooth surface viscous impeller pump rotating at 5000 rpm. SVC, Superior vena cava; IVC, inferior vena cava, LPA, left pulmonary artery; RPA, right pulmonary artery.[51]Reproduced with permission from Rodefeld et al. *J Thorac Cardiovasc Surg*, 2010, 140, 529-36.

CONCLUSIONS

Since its first description nearly forty years ago, the Fontan operation has undergone many modifications with an aim to have a longer event free palliation and to improve the functional status of these patients. Needless to say, many of these modifications have been made because of a better understanding of the fluid dynamics, energy losses and multiple in-vivo and in-vitro experiments. Computational fluid dynamics which can create accurate models of the various modifications of this operation has contributed significantly towards achieving the ever elusive goal of an “ideal Fontan”. Current research is now focused over designing various artificial pumps which can add energy to this abnormal state so that it can function for a longer period of time. It is anticipated that using the principles of fluid dynamics, it may be possible to design compact and easily implantable pumps that may obviate the need for heart transplantation for a failing Fontan circuit.

REFERENCES

1. Fontan FBE. Surgical repair of tricuspid atresia. *Thorax*, 1971, 26, 240–248.
2. Fontan FDC, Quaegebeur JM, Ottenkamp J, Sourdille N, Choussat ABG. Repair of tricuspid atresia in 100 patients. *J Thorac Cardiovasc Surg*, 1983, 85, 647–660.
3. Kreutzer GGE, Bono H, De Palma C, Laura JP. An operation for the correction of tricuspid atresia. *J Thorac Cardiovasc Surg*, 1973, 6, 13–621.

4. de Leval MR, Kilner P, Gewillig M, Bull C .Total cavopulmonary connection: A logical alternative to atriopulmonary connection for complex Fontan operations :Experimental studies and early clinical experience. *J Thorac Cardiovasc Surg*, 1988, 96, 682–695.
5. de Leval MR. The Fontan circulation: a challenge to William Harvey? *Nat Clin Pract Cardiovasc Med*, 2005, 2 (4), 202-8.
6. Puga FT CM, Hagler DJ. Modifications of the Fontan operation applicable to patients with left atrioventricular valve atresia or single atrioventricular valve. *Circulation*, 1987, 76 (III) 53–60.
7. Pediatric cardiac surgery, MAVROUDIS, BECKER CARL 3 rd edition.
8. Cheung YF, Penny DJ, Redington AN. Serial assessment of left ventricular diastolic function after Fontan procedure. *Heart*, 2000, 83, 420–424.
9. Nogaki M, Senzaki H, Masutani S, Kobayashi J, Kobayashi T, Sasaki N, Asano H, Kyo S, Yokote Y. Ventricular energetics in Fontan circulation: evaluation with a theoretical model. *Pediatrics International*, 2000, 42, 651–657.
10. Senzaki H, Masutani S, Kobayashi J, Kobayashi T, Sasaki N, Asano H, Kyo S, Yokote Y, Ishizawa A. Ventricular afterload and ventricular work in Fontan circulation: Comparison with normal two-ventricle circulation and single ventricle circulation with Blalock-Taussig shunts. *Circulation*, 2002, 105, 2885–2892.
11. Szabó G, Buhmann V, Graf A, Melnitschuk S, Bährle S, Vahl CF, Hagl S. Ventricular energetics after the Fontan operation: contractility-afterload mismatch. *J Thorac Cardiovasc Surg*, 2003, 125, 1061–1069.
12. Kussmaul WG, Noordergraaf A, Laskey WK. Right ventricular-pulmonary arterial interactions. *Ann Biomed Eng*, 1992, 20, 63–80.
13. Milnor NR. Pulmonary hemodynamics. In *Cardiovascular fluid-dynamics*, Ed. Bergel DH, Academic Press, London, 1972, 2, 299–340.
14. Feldt R, Driscoll D, Offord K, Cha R, Perrault J, Schaff H. Protein-losing enteropathy after the Fontan operation. *J Thorac Cardiovasc Surg*, 1996, 112, 672–680.
15. Gentles TL, Gauvreau K, Mayer JE Jr, Fishberger SB, Burnett J, Colan SD, Newburger JW, Wernovsky G. Functional outcome after the Fontan operation: factors influencing late morbidity. *J Thorac Cardiovasc Surg*, 1997, 114, 392–403.
16. Hug MI, Ersch J, Moenkhoff M, Burger R, Fanconi S, Bauersfeld U. Chylous bronchial casts after Fontan operation. *Circulation*, 2001, 103, 1031–1033.
17. Triedman JK, Bridges ND, Mayer JE Jr, Lock JE. Prevalence and risk factors for aortopulmonary collateral vessels after Fontan and bidirectional Glenn procedures. *J Am Coll Cardiol*, 1993, 22, 207–215.
18. Srivastava D, Preminger T, Lock JE, Mandell V, Keane JF, Mayer JE Jr, Kozakewich H, Spevak PJ. Hepatic venous blood and the development of pulmonary arteriovenous malformations in congenital heart disease. *Circulation*, 1995, 92, 1217–1222.
19. Ensley AE, Lynch P, Chatzimavroudis GP, Lucas C, Sharma S, Yoganathan AP. Toward designing the optimal total cavopulmonary connection: an in vitro study. *Ann Thorac Surg*, 1999, 68, 1384–1390.
20. Gerdes A, Kunze J, Pfister G, Sievers HH .Addition of a small curvature reduces power losses across total cavopulmonary connections. *Ann Thorac Surg*, 1999, 67, 1760–1764.
21. Sharma S, Goudy S, Walker P, Panchal S, Ensley A, Kanter K, Tam V, Fyfe D, and Yoganathan A. In vitro flow experiments for determination of optimal geometry of total cavopulmonary connection for surgical repair of children with functional single ventricle. *J. Am. Coll. Cardiol*, 1996, 27, 1264-1269.
22. Hsia T Y, Khambadkone S, Deanfield J E, Taylor J F, Migliavacca F, and de Leval M R. Subdiaphragmatic venous hemodynamics in the Fontan circulation. *J. Thorac. Cardiovasc. Surg*, 2001, 121, 436-447.
23. DeGroff C G, Carlton J D, Weinberg C E, Ellison M C, Shandas R, and Valdes-Cruz L. Effect of vessel size on the flow efficiency of the total cavopulmonary connection: In vitro studies. *Pediatr. Cardiol*, 2002, 23, 171-177.

24. Sharma S, Ensley A E, Hopkins K, Chatzimavroudis G P, Healy, T M, Tam, V. K., Kanter, K. R., and Yoganathan A P. In vivo flow dynamics of the total cavopulmonary connection from three-dimensional multislice magnetic resonance imaging. *Ann. Thorac. Surg*, 2001, 71, 889-898.
25. Fogel M A, Weinberg P M, Rychik J, Hubbard A, Jacobs M, Spray T L, and Haselgrove J. Caval contribution to flow in the branch pulmonary arteries of Fontan patients with a novel application of magnetic resonance presaturation pulse. *Circulation*, 1999, 99, 1215-1221.
26. Gerdes A, Hanke T, Ahrens V, Pfister G, and Sievers H H. Does caval aplanarity influence power losses across in vitro cavopulmonary connections? *Pediatr. Cardiol*, 2002, 23, 388-393.
27. Fontan F, Kirklin JW, Fernandez G, Costa F, Naftel DC, Tritto F, Blackstone EH. Outcome after a “perfect” Fontan operation. *Circulation*, 1990, 81, 1520–1536.
28. de Zelicourt DA, Pekkan K, Wills L, Kanter K, Forbess J, Sharma S, Fogel M, Yoganathan AP. In vitro flow analysis of a patient-specific intraatrial total cavopulmonary connection. *Ann Thorac Surg*, 2005, 79, 2094–2102.
29. DeGross C, Birnbaum B, Shandas R, Orlando W, Hertzberg J. Computational simulations of the total cavopulmonary connection: Insights in optimizing numerical solutions. *Med Eng Phys*, 2005, 27, 135– 146.
30. DeGross CG, Carlton JD, Weinberg CE, Ellison MC, Shandas R, Valdes-Cruz L. Effect of vessel size on the flow efficiency of the total cavopulmonary connection: In vitro studies. *Pediatr Cardiol*, 2002, 23, 171–177.
31. DeGross CG, Shandas R. Designing the optimal total cavopulmonary connection: Pulsatile versus steady flow experiments. *Med Sci Monitor*, 2002, 8, MT41–MT45.
32. Migliavacca F, Dubini G, deLeval MR. Computational fluid dynamics in paediatric cardiac surgery. *Images Paediatr Cardiol*, 2000, 2, 11-25.
33. Moreno AH, Katz AI, Gold LD. An integrated approach to the study of the venous system with steps toward a detailed model of the dynamics of venous return to the right heart. *IEEE Trans Biomed Eng*, 1969, 16, 308-324.
34. Bove EL, de Leval MR, Migliavacca F, Guadagni G, Dubini G. Computational fluid dynamics in the evaluation of hemodynamic performance of cavopulmonary connections after the Norwood procedure for hypoplastic left heart syndrome. *J Thorac Cardiovasc Surg*, 2003, 126, 1040-1047.
35. Hsia T-Y, Migliavacca F, Pittaccio S, Radaelli A, Dubini G, Pennati G, de Leval M. Computational fluid dynamic study of flow optimization in realistic models of the total cavopulmonary connections. *J Surg Res*, 2004, 116, 305–313.
36. Lardo AC, Webber SA, Friehs I, del Nido PJ, Cape EG. Fluid dynamic comparison of intraatrial and extracardiac total cavopulmonary connections. *J Thorac Cardiovasc Surg*, 1999, 117, 697-704.
37. Migliavacca F, de Leval MR, Dubini G, Pietrabissa R, Fumero R. Computational fluid dynamic simulations of cavopulmonary connections with an extracardiac lateral conduit. *Med Eng Phys*, 1999, 21, 187–193.
38. Ascuitto RJ, Kydon DW, Ross-Ascuitto NT. Pressure loss from flow energy dissipation: Relevance to Fontan-type modifications. *Pediatr Cardiol*, 2001, 22, 110–115.
39. Ascuitto RJ, Kydon DW, Ross-Ascuitto NT. Streamlining fluid pathways lessens flow energy dissipation: Relevance to atriocavopulmonary connections. *Pediatr Cardiol*, 2003, 24, 249–258.
40. de Leval MR, Dubini G, Migliavacca F, Jalali H, Camporini G, Redington A, Pietrabissa R. Use of computational fluid dynamics in the design of surgical procedures: Application to the study of competitive flows in cavopulmonary connections. *J Thorac Cardiovasc Surg*, 1996, 111, 502–513.
41. De Zelicourt DA, Pekkan K, Wills L, Kanter K, Forbess J, Sharma S, Fogel M, Yoganathan AP. In vitro flow analysis of a patient-specific intraatrial total cavopulmonary connection. *Ann Thorac Surg*, 2005, 79, 2094–2102.
42. Dubini G, de Leval MR, Pietrabissa R, Montevecchi FM, Fumero R. A numerical fluid mechanical study of repaired congenital heart defects: Application to the total cavopulmonary connection. *J Biomech*, 1996, 29, 111–121.

43. Ensley AE, Lynch P, Chatzimavroudis GP, Lucas C, Sharma S, Yoganathan AP Toward designing the optimal total cavopulmonary connection: An in vitro study. *Ann Thorac Surg*, 1999, 68, 1384–1390.
44. Gerdes A, Kunze J, Pfister G, Sievers HH Addition of a small curvature reduces power losses across total cavopulmonary connections. *Ann Thorac Surg*, 1999, 67, 1760–1764.
45. Grigioni M, D’Avenio G, Del Gaudio C, Morbiducci U. Critical issues in studies of flow through the Fontan circuit after 10 years of investigation. *Cardiol Young*, 2005, 15 (Suppl 3), 68–73.
46. Masters JC, Ketner M, Bleiweis MS, Mill M, Yoganathan A, Lucas CL . The effect of incorporating vessel compliance in a computational model of blood flow in a total cavopulmonary connection (TCPC) with caval centerline offset. *J Biomech Eng*, 2004, 126, 709–713.
47. Migliavacca F, de Leval MR, Dubini G, Pietrabissa R, Fumero R Computational fluid dynamic simulations of cavopulmonary connections with an extracardiac lateral conduit. *MedEng Phys*, 1999, 21, 187–193.
48. Khunatorn Y, Mahalingam S, DeGroof CG, Shandas R Influence of connection geometry and SVC–IVC flow rate ratio on flow structures within the total cavopulmonary connection: Anumerical study. *J Biomech Eng*, 2002, 124, 364–377.
49. Kim SH, Park YH, Cho BK . Hemodynamics of the total cavopulmonary connection: An in vitro study. *Yonsei Med J*, 1997, 38, 33–39.
50. Amodeo A, Grigioni M, D’Avenio G, Daniele C, Di Donato RM The patterns of flow in the total extracardiac cavopulmonary connection. *Cardiol Young*, 2004, 14 (Suppl 3), 53–56.
51. Rodefeld MD, Coats B, Fisher T, Giridharan GA, Chen J, Brown JW, Frankel SH Cavopulmonary assist for the univentricular Fontan circulation: von Kármán viscous impeller pump *J Thorac Cardiovasc Surg*, 2010 Sep, 140 (3), 529-536.

